Research Square

Preprints are preliminary reports that have not undergone peer review.
They should not be considered conclusive, used to inform clinical practice,
or referenced by the media as validated information.

Incremental-power-based improved protection algorithm for HVDC transmission line protection

Soma Deb

soma.deb@sharda.ac.in

Sharda University

Abhay Yadav

Sharda University

Sumanlata Dhar

Sharda University

Research Article

Keywords: AC fault, DC fault, fault detection, fault classification, incremental-power, HVDC system, PSCAD, signum function

Posted Date: November 20th, 2026

DOI: https://doi.org/10.21203/rs.3.rs-11399838/v1

License: This work is licensed under a Creative Commons Attribution 4.0 International License.
Read Full License

Additional Declarations: No competing interests reported.

Incremental-power-based improved protection algorithm for HVDC transmission line protection

Soma Deb[1] , Abhay Yadav[1] and Sumanlata Dhar[1]

[1] Electrical and Electronics and Communication Engineering Department, Sharda School of Engineering and Science, Sharda University, Greater Noida, Uttar Pradesh, India

(Email Address of the Corresponding Author: soma.deb@sharda.ac.in)

Abstract: We developed an improved approach for fault recognition and classification based on the signum function of incremental power, using synchronized data collected at both HVDC line terminals during a fault. The proposed algorithm is tested and evaluated for faults with different fault resistance values. The HVDC benchmark system created by CIGRE was used to validate the approach. The proposed algorithm was evaluated for performance using PSCAD/EMTDC simulations. The simulation results display five fault locations and five fault resistance values. The signum function was then used to analyze the simulation data and assess the proposed strategy's efficacy for fault detection and classification. The proposed algorithm provides ultra-fast protection, enabling detection and classification of all internal and external faults across a wide range of fault resistance values in less than 3 milliseconds.

Keywords: AC fault; DC fault; fault detection; fault classification; incremental-power; HVDC system; PSCAD; signum function

1. Introduction

Modern power systems increasingly use high-voltage direct current (HVDC) transmission systems due to rapid advances in power electronic converters and their control mechanisms [1], [2]. The traditional AC power system has not fully met the needs of large-scale renewable energy consumption, despite advances in renewable energy access capacity. HVDC transmission technology is an efficient option, offering controllable power flow, lower transmission losses over long distances, reduced right-of-way requirements, and suitability for integrating remote renewable energy

resources. Selecting appropriate electrical, insulation, conductor, and converter materials is also important for maintaining system reliability [3].

Generating, transmitting, and distributing electrical power require substantial capital investment in equipment, materials, and associated infrastructure. Therefore, proper precautions must be taken to keep power system components operating as close to peak efficiency as possible and protected from faults and accidents. In an HVDC transmission line, the protection system's primary purpose is to trigger DC line protection, which blocks both the converter and inverter, preventing power flow through the DC line before resulting electrical and thermal stresses cause permanent damage to equipment or materials.

Faults in HVDC transmission lines cause a rapid rise in DC fault current and a collapse of DC voltage, creating technical challenges for fault detection and classification. These transients impose severe electrical and thermal stresses on transmission line materials, converters, conductors, and other associated components. Fault recognition and classification must occur as quickly as possible to minimize the impact of faults on the HVDC system. Hence, a very fast and reliable protection algorithm is required. The following are some of the technical challenges of LCC-based HVDC system protection:

i. DC fault current has no natural zero crossing as in the case of AC. This is the main challenge in developing HVDC circuit breakers, as mechanical circuit breakers require a natural zero-crossing to interrupt fault current. The absence of zero crossing places additional stress on dielectric materials used in insulation.

ii. The use of high-voltage DC circuit breakers is not suitable in LCC-based HVDC systems because the energy driven by the DC fault needs to be dissipated by the breakers themselves, making the circuit breaker more complex in terms of design and maintenance for high-current-rated LCC-based HVDC transmission systems. This complexity increases further because robust breaker materials must withstand repeated fault stresses.

iii. The impedance of the DC transmission line is significantly lower, which results in larger fault current values for a DC fault. Such rapid current escalation can impose significant electromagnetic and thermal stresses on conductors, insulation materials, converter components, and other equipment.

Fault occurrence in HVDC transmission lines is much more likely compared with any other element of the HVDC transmission system [4], [5]. This is because of the long length of the lines and the rough topography they generally pass through. In addition, fault current in a DC transmission

line can reach very high, dangerous levels very quickly because the DC system has relatively low impedance [6]. This rapid fault-current rise increases the thermal and electrodynamic stresses on conductors and other line materials. An HVDC transmission system has a large series inductance, called the smoothing reactor, at both ends of the DC line to suppress ripple current. In addition, the HVDC system has significant shunt capacitance due to DC filters at both ends, where dielectric materials play a critical role in performance. The system must dissipate energy stored in the series inductance and shunt capacitance to interrupt the fault current. In addition, fault current will be fed from the AC system itself during a fault on a DC line. This results in significant energy dissipation, which may damage the converter circuit and insulation materials if the fault is not detected quickly enough [7],[8],[9],[31]. A fast protection technique is therefore equally crucial, given the fault's severity and the limitations of conductor materials under repeated stress.

Conventional protection systems that are reported in the literature can be grouped into (i) traveling wave-based protection, (ii) differential protection, (iii) under-voltage protection, and (iv) protections based on voltage and current derivatives [10],[11],[12],[13],[14]. These protection techniques have drawbacks, such as reduced sensitivity as fault resistance increases, susceptibility to noise and disturbances, the need for very high sampling rates, and low operating speed. However, within these constraints, a comprehensive literature survey has examined how dielectric materials affect fault-detection accuracy.

In one traveling-wave-based protection technique reported in the literature, the authors developed a protection algorithm that used features of forward- and backward-traveling waves [15]. In this technique, the authors used the features of backward-traveling waves that were balanced at both ends of the HVDC transmission line. In contrast, internal faults were detected because they caused the backward-traveling waves to become imbalanced. Unlike traditional current differential protection, the proposed protection principle eliminated the impact of distributed capacitive current and required no delay [16]. In addition, unlike traditional traveling-wave-based protection, this approach can detect faults under both transient and steady-state conditions. This approach requires a low sampling frequency. The authors did not present any reliability analysis or examine the role of insulating materials. Recently, two traveling-wave-based protection algorithms were proposed in [17] and [18]. These approaches relied solely on the first incident-induced traveling wave and neglected the wavefront originating at the fault point. Although the protection approach was more accurate, it was unreliable because the authors did not account for fault resistance or variability in conductor materials.

Various papers in the literature have used current or certain components of current as the protection variable. In [19], the authors report a novel incremental-current-based protection scheme. Compared with traditional traveling-wave and wavelet-based approaches, this technique offers improved reliability and practicality while relying less on communication infrastructure. This work contributes significantly to HVDC protection research by highlighting scalability challenges and the potential for real-world deployment in modern power grids, where conductor and insulation materials directly affect system resilience.

[20] also reported a fault detection approach based on transient energy. Compared with conventional traveling-wave and wavelet-based approaches, this study highlights enhanced reliability, practicality, and potential for real-world HVDC grid protection, with an emphasis on dielectric durability.

A protection technique based on current harmonic components has been reported in [21]. Converter operation generated characteristic harmonic currents at the 12th-, 24th-, and 36th-order in the DC transmission line. In this technique, these harmonic currents were extracted using Discrete Fourier Transform (DFT). A DC filter unit was installed at both ends of the DC line, between the converter and the protection unit. During external AC faults, the filter unit blocked the generation of characteristic harmonic currents by both the faults and the converters. The protection unit therefore did not capture them. During a DC internal fault, the DC filter unit readily captured these characteristic harmonic currents, enabling detection of DC line faults. This approach had certain limitations. Higher fault resistance values resulted in reduced sensitivity. Fault location also affected the protection scheme's sensitivity. Sensitivity decreased further for faults at the far end of the DC line, where conductor and insulation materials degrade signal clarity.

The converter transformer's inrush condition may unintentionally trigger the HVDC protection system. [22] proposed a protection technique using current-restraint and voltage parameters. In this approach, the 2^{nd} harmonic component was extracted from the DC line current to detect inrush and inhibit protection triggering under inrush conditions. In [23], a protective strategy based on transient voltage properties was proposed. This analysis focused on the characteristic function of the entire unit, which included the DC filter, DC line, and smoothing reactor. This feature served as the foundation for fault identification and categorization because it differed between internal and external faults. The author assessed the algorithm's performance only for fault resistance up to 500 ohms, without considering the role of dielectric materials.

China's primary HVDC protection systems were based on non-unit traveling-wave protection principles from SIEMENS and ABB. ABB used a polar-wave derivative (dp/dt) and a voltage derivative (dv/dt) to detect faults in an HVDC transmission line [24]. Both had reduced sensitivity as fault resistance increased [25]. [26] evaluated four traveling-wave approaches. This paper considered both frequency-dependent and frequency-independent line models. The paper discussed the main sources of error and accuracy for all four approaches and explained each approach's practical applications. The single-terminal traveling-wave fault location method was another traveling-wave-based fault identification method. The technique relied on calculations and measurements of arrival times, that is, the arrival times of the initial incident traveling wave and reflections from the fault terminal and the remote terminal. Differentiating traveling waves, whether refracted or reflected from a fault point or through other components or materials in a power system, was the major challenge of this approach and may hinder the fault locator's reliability [27], [28]. Another traveling wave-based protection algorithm was recently proposed in [29]. The proposed technique distinguishes between transmission-line faults and line-terminal faults. In addition, this approach eliminated the need to estimate the traveling-wave propagation speed. However, the evaluation did not consider fault resistance or the effects of conductor material.

Protection principles based on boundary principles are easily affected by fault current limiting reactors (FCLRs) and therefore fail to identify all fault conditions [30]. The performance of these schemes is also influenced by the dielectric materials used in insulation and magnetic materials used in reactors.

[31] presented a distributed-parameter-based DC line protection technique that uses common- and differential-mode compensation currents to select faulty poles. This method's performance is independent of the distributed capacitance current; however, the proposed scheme depends heavily on system characteristics, including the resistive and capacitive properties of line materials, and the computational procedure is complex.

In [32], a data-driven protection plan was developed that leverages the XGBoost machine learning (ML) algorithm. One benefit of this technique is that it eliminates the need to establish the protection threshold. [33] proposed a non-unit protection strategy for VSC-HVDC lines based on waveform similarity and the wavelet transform modulus maximum (WTMM) theory. Remote faults and excessive fault resistance can be detected using this protection technique. Additionally, it is unaffected by start delay, smoothing reactors, signal noise, and sampling frequency, although material electromagnetic properties still play a role. In [34], a DC line protection technique based

on active injection was presented; however, the active injection device increased operational risk due to stress on insulation materials. These techniques provide strong protection, but they are not suitable for LCC-VSC hybrid HVDC gearbox systems because they require long fault-information processing times and are sensitive to conductor materials.

High-impedance faults in hybrid HVDC transmission lines can cause conventional protection schemes to misoperate. [35] proposed a single-ended protection technique that coordinates control objectives to improve sensitivity to high-resistance faults. This approach extracts fault signatures from the DC line current and voltage, enabling reliable detection without requiring communication links. However, noise interference, long-distance transmission effects, and variability in line materials limit performance.

In [36], the authors introduced a protective strategy for large-scale MMC-HVDC systems that combines DC circuit breakers with fault current limiters. This hybrid approach reduces breaker stress and energy absorption during fault clearing, thereby improving system reliability. The authors showed that coordinated breaker and limiter operation significantly improves fault-current handling, though it increases system complexity, cost, and reliance on durable materials for breaker design.

In [37], the authors proposed a method based on traveling-wave theory and the Hilbert transform for fault detection, classification, and localization. In [37], the authors proposed a method based on traveling-wave theory and the Hilbert transform for fault detection, classification, and localization. The analysis showed that the Hilbert transform improves fault-type discrimination accuracy but requires high sampling rates. Researchers have also explored adaptive signal processing techniques, with attention to their interaction with conductor materials.

In [38], an adaptive thresholding method was proposed to enhance HVDC fault detection under noisy conditions. The algorithm dynamically adjusts detection thresholds based on signal characteristics, improving sensitivity to high-impedance faults. In [39], a novel scheme based on the line-mode current-time warp edit distance (TWED) was introduced. This approach demonstrated robustness to noise and effective detection across varying fault resistances, though it required offline parameter tuning and careful calibration of insulation materials.

[41] highlighted protection challenges in multi-terminal HVDC (MTDC) networks and reviewed offshore energy integration strategies. The study emphasized the need for standardized protection schemes and vendor interoperability. Complementary to this, [42] discussed HVDC

circuit breaker technologies and interoperability challenges, identifying hybrid breakers as the most promising solution. [43] provided a broader review of HVDC circuit breaker research, comparing mechanical, solid-state, and hybrid designs and concluding that hybrid breakers offer the best trade-off between speed and efficiency. However, they remain immature for large-scale deployment, partly due to limitations in available materials.

Finally, [44] investigated single-ended fault location methods incorporating traveling waves. This approach reduced hardware costs by operating at lower sampling rates, but its accuracy diminished when traveling-wave signals were weak or when line materials introduced distortion.

All these protection schemes reported in the literature and reviewed above have the common feature that they are based on communicating the measured values of certain system variables (like instantaneous magnitudes and signs of voltage, current, power, etc.) from the remote end of the transmission line to the local end, which can take a long communication time, thereby delaying the decision as to whether the fault is internal or external. Therefore, this approach compares only the signs (polarities) of the selected system variables, not their magnitudes. The time required to send only the sign (positive or negative) will be much shorter than the time needed to send the magnitude along with a sign. Therefore, this paper develops an improved fault detection and classification algorithm for HVDC system protection that uses the signum function of incremental power to quickly detect and classify faults while accounting for the influence of conductor and insulation materials.

This paper proposes an improved fault detection and classification algorithm using the signum function of incremental power. Section II presents the simulation model of the HVDC transmission system with PDTF, followed by the proposed protection algorithm in Section III. Section IV presents simulation results for the protection algorithm, followed by a performance evaluation in Section V. Section VI summarizes and concludes the proposed protection algorithm, highlighting the importance of robust materials in ensuring reliability.

2. Simulation Model of HVDC Transmission System with PDTF

In this paper, we implement the HVDC transmission test setup in PSCAD/EMTDC for simulation. The benchmark system is the CIGRE benchmark system [45]. Researchers have used PSCAD/EMTDC to model HVDC systems in various research papers [46], [47]. Fig. 1 (a) shows the simulation model of an HVDC transmission system with PDTF. The line has a 500 kV voltage rating and a 2 kA current rating. It is 800 kilometers long. The line is modeled with frequency-dependent

parameters that incorporate conductor and insulation materials to represent realistic transmission behavior. The AC system power frequency is set to 50 Hz, and the sampling frequency is 2 kHz.

To prevent harmonic currents from entering the DC line, we install DC filters at both ends. In this simulation model, we use a parallel double-tuned filter (PDTF), as shown in Fig. 1(b). This filter is comprised of a 12/24 type filter, which means that it is tuned to the 12th and 24th order harmonics of the fundamental frequency (i.e., 600 Hz and 1200 Hz), connected in parallel with a 12/36 type filter, tuned to the 12th and 36th order harmonics of the fundamental frequency (i.e., 600 Hz and 1800 Hz) [48]. The component values are given below, highlighting the role of dielectric materials in capacitors, magnetic materials in inductors, and structural materials in filter housing.

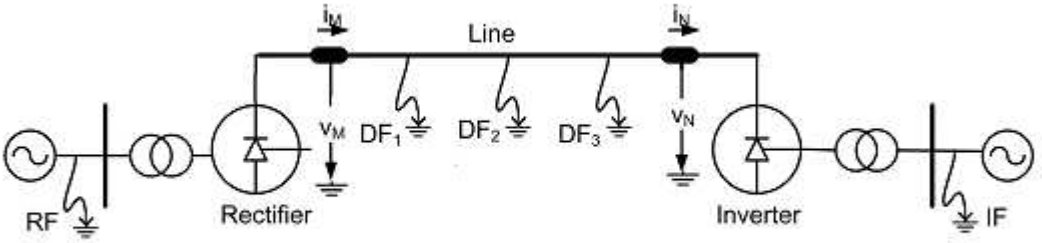
$L_{d1} = 0.29$ H

$C_1 = 2\mu F$, $L_1 = 11.71mH$

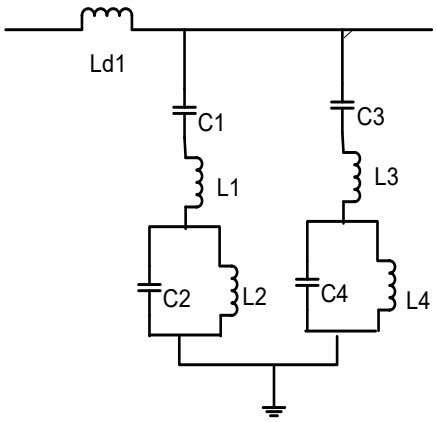
$C_2 = 9.074\mu F$, $L_2 = 5.874mH$

$C_3 = 2\mu F$, $L_3 = 6.46mH$

$C_4 = 3.752\mu F$, $L_4 = 11.35mH$



(a)



(b)

Figure 1. HVDC Transmission Test System
(a) Simulation Model (b) DC filter

Measurement devices for instantaneous direct current and voltage were placed at both ends, M and N, of the DC transmission line. RF and IF here denote solid three-phase AC faults on the rectifier and inverter ends, respectively. DF_1, DF_2, and DF_3 represent DC faults at the sending end, midpoint, and receiving end of the line, respectively. The five faults were created sequentially at 0.500 s. Measurement data (instantaneous voltage values, V_M and V_N, and instantaneous current values, I_M and I_N, at the two ends M and N) were recorded over one power cycle (40 samples @ 2 kHz) before the inception of the fault (over 0.4800 - 0.4995 s) and two power cycles (80 samples @ 2 kHz) after the fault inception (over 0.500 - 0.5395 s).

3. Proposed Protection Algorithm

The incremental power-based protection algorithm uses the signum function of the change in incremental power computed at both ends of the DC transmission line. The system model utilized to analyze the method is as shown in Fig. 1.

Variation in incremental power from time 0 to t can be expressed as

$$\Delta P_M = \int_0^t \Delta V_M . \Delta I_M . dt \quad (1)$$

$$\Delta P_N = \int_0^t \Delta V_N . \Delta I_N . dt \quad (2)$$

In discrete form, equations 1 and 2 can be written as

$$\Delta P_M = \sum_{k=0}^{n} \Delta V_{Mk} \Delta I_{Mk} \quad (3)$$

where,

ΔV_{Mk} = increment of DC voltage at the kth instant at point M

ΔI_{Mk} = increment of DC at the kth instant at point M

Similarly

$$\Delta P_N = \sum_{k=0}^{n} \Delta V_{Nk} . \Delta I_{Nk} \quad (4)$$

ΔV_{Nk}= increment of DC voltage at the kth instant at point N

ΔI_{Nk} = increment of DC at the kth instant at point N

For any random variable a, sgnum(a) can be written as under [49]:

$$\text{signum}(a) = \begin{cases} -1 \text{ when } a < 0 \\ 0 \text{ when } a = 0 \\ 1 \text{ when } a > 0 \end{cases} \quad (5)$$

In the end, the summation of the signum function (ssgnum) is obtained using the equation below:

$$\text{ssgnum} = \text{sgnum}(\Delta P_M) + \text{sgnum}(\Delta P_N) \quad (6)$$

Under no-fault conditions, both ΔPM and ΔPN remain zero, so their signum functions, as well as their sum (ssgnum), remain zero. In the event of any internal DC line fault, there will be opposing signs and non-zero values for both ΔP_M and ΔP_N. The sum (ssgnum) will therefore be zero, since one has a signum function of +1 and the other of -1. The values of ΔP_M and ΔP_N will both be non-zero and have the same sign when there is an external AC fault. The signum functions sgnum(ΔP_M) and sgnum(ΔP_N) will take the values +1 and -1, respectively. Consequently, their sum will be either +2 or -2.

The protection algorithm shown in Fig. 2 is used to evaluate the proposed algorithm's performance. The algorithm receives the voltage and current at both ends M and N, along with time, fed continuously and synchronously. Following this, the signum of the variation in incremental power at either end is obtained from the recorded voltage and current values at that end. According to the principle, if the signum functions of ΔP_N and ΔP_M are both zero, the system is in a no-fault condition. As a result, the algorithm uses the next set of voltage and current samples, as indicated by the flowchart. A fault is indicated when the specified criteria are not met. Next, we compute the ssgnum for the incremental power variations at both ends of a line. After that, the fault is classified using this value, and the next set of steps is as follows:

a. The algorithm returns to get the subsequent batch of input samples if ssgnum ≠ 0—an indication of an external AC fault.
b. The algorithm returns to get the subsequent batch of input samples if ssgnum = 2—an indication of a rectifier-side AC line fault.
c. The algorithm returns to get the subsequent batch of input samples if ssgnum= -2—an indication of an inverter-side AC line fault.
d. The algorithm triggers the DC line protection if ssgnum = 0—an indication of an internal DC line fault

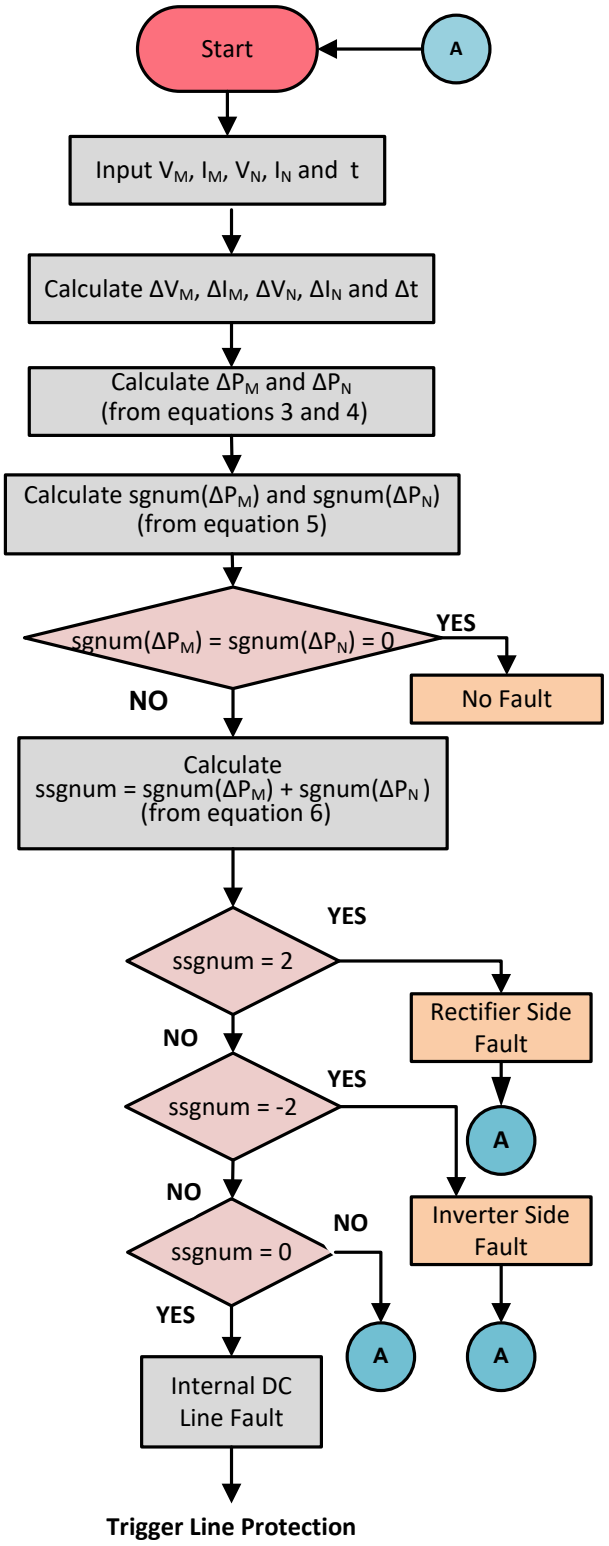


Figure 2. Protection Algorithm

4. Simulation Results

To evaluate the performance of the proposed protection algorithm in terms of incremental power, we obtained simulation results for all five locations and all five fault resistance values, as shown below.

4.1 Rectifier-side DC fault (DF_1)

Fig. 3 illustrates changes in incremental power at the two ends, ΔP_M and ΔP_N, over time for the rectifier-end DC fault (DF_1). Figs. 3 (a) to (e) show that ΔP_M has negative values and ΔP_N has positive values for at least half an AC power cycle (10 ms) for all fault resistance values in the range of 0 ohms to 2000 ohms. The incremental-power change at end N shows a 3 ms delay, as observed from the incremental-power curve ΔP_N.

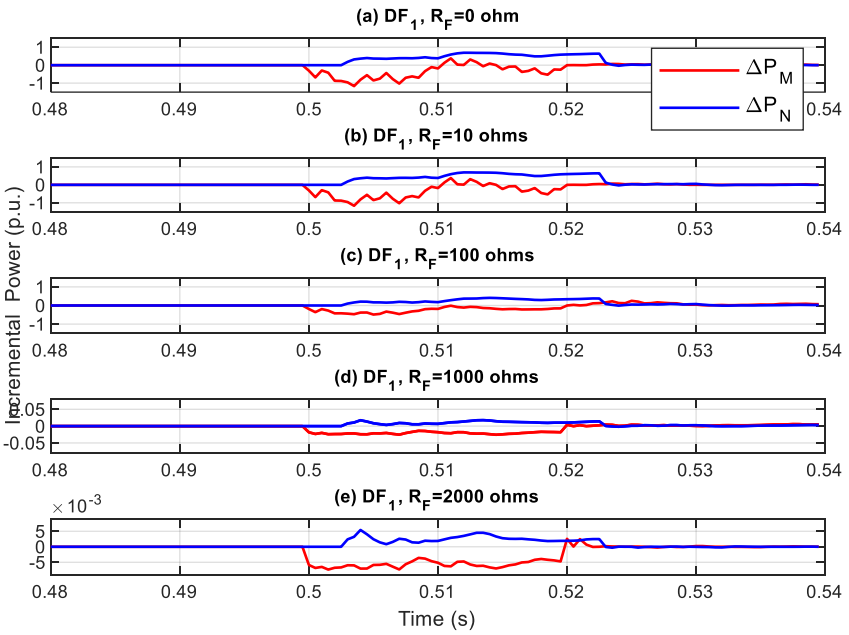


Figure 3. Incremental-power response curves for DF_1

4.2 Mid-point DC fault (DF_2)

Fig. 4 shows the changes in incremental power, ΔP_M and ΔP_N for the mid-point DC fault (DF_2).

For all fault resistance values, ΔP_M is negative and ΔPN is positive for at least 20 ms, as shown in Fig. 4(a)-(e). Based on Fig. 4, the incremental-power response shows a 1.5 ms delay for both ΔP_M and ΔP_N.

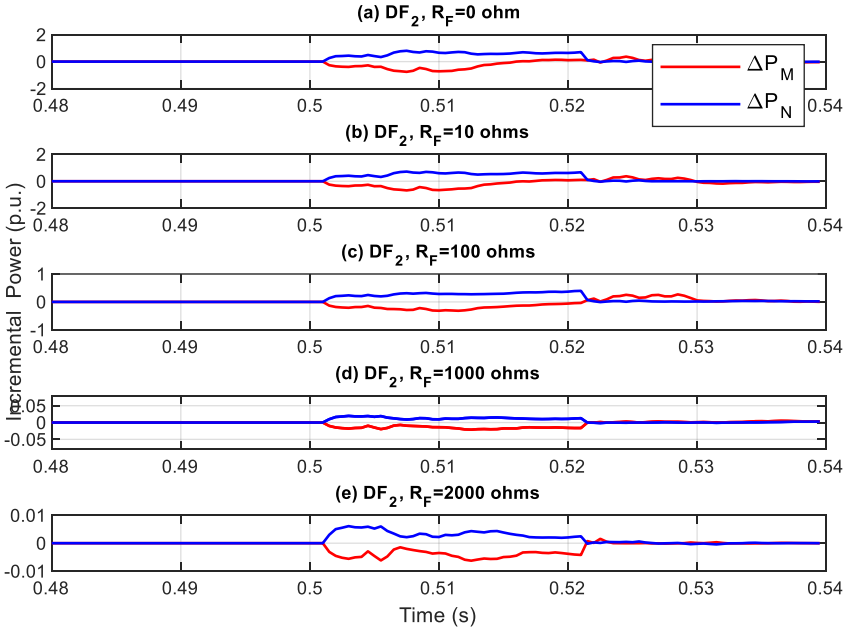


Figure 4. Incremental power response curves for DF_2

4.3 Inverter-side DC fault (DF_3)

Fig. 5 shows changes in incremental power at the two ends, ΔP_M and ΔP_N, over time for the inverter-side DC fault (DF_3). Figs. 5(a)-(e) show that ΔPM is positive and ΔPN is negative for at least half an AC power cycle (10 ms) for all fault resistance values.

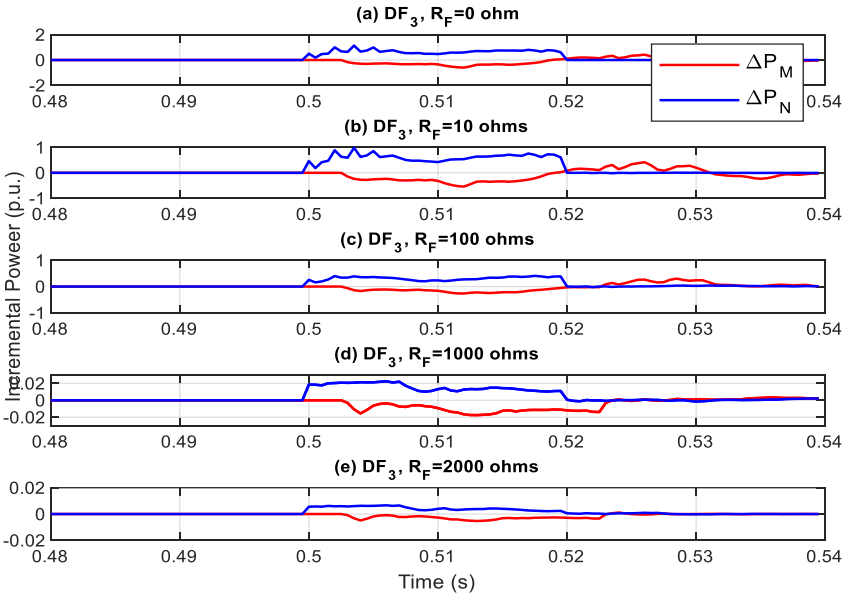


Figure 5. Incremental-power response curves for DF_3

4.4 Rectifier-side AC fault(RF)

As shown in Fig.6, incremental-power response curves, $\Delta P_{M,}$ and ΔP_N are positive for at least a 20 ms period following the onset of the fault for inverter-side external fault IF.

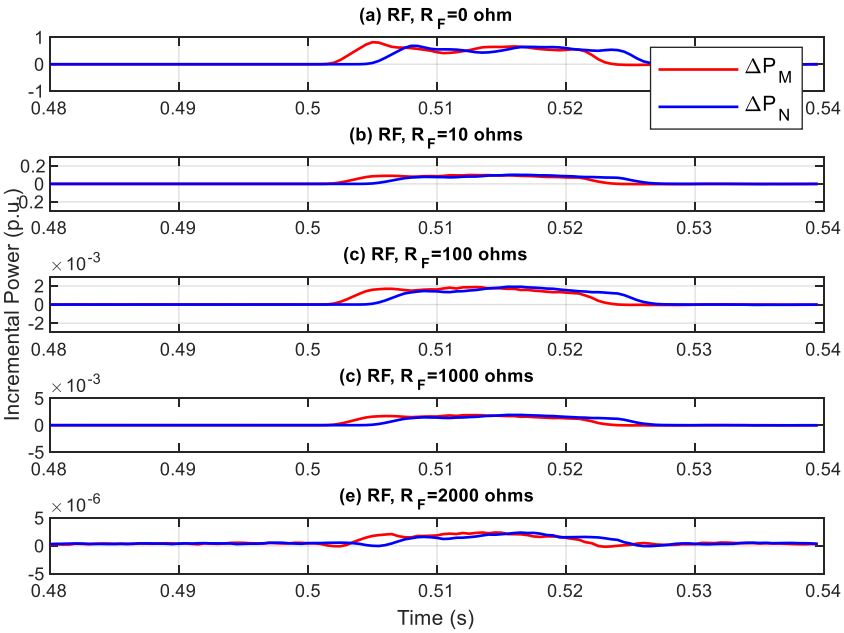


Figure 6. Incremental-power Response Curves for RF

4.5 Inverter-side external fault (IF)

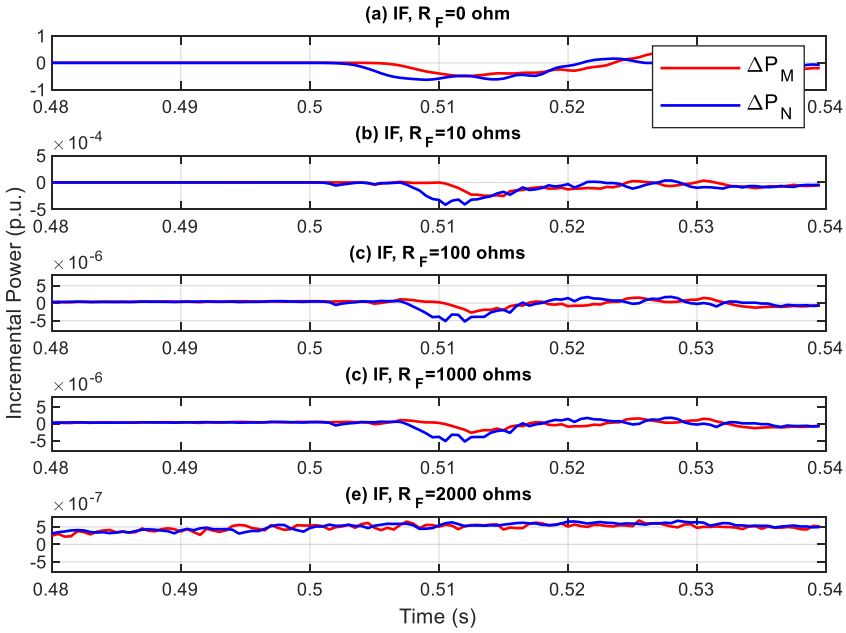


Figure 7. Incremental-power Response Curves for IF

As shown in the incremental power curves of Fig. 7(a) to (d) for fault resistance values from 0 ohms to 1000 ohms, ΔPM and ΔP_N both turn negative and stay that way for at least a 20 ms period following the onset of the fault. In contrast, Fig. 7(e) shows that for a fault resistance of 2000 ohms, ΔPM and ΔPN both turn positive and remain positive for at least 20 ms after the fault onset.

5. Performance Evaluation

The algorithm's performance has been thoroughly evaluated for fault occurrences at all locations along the line, across a spectrum of fault resistance values, and is presented below:

5.1 Rectifier-side DC fault (DF_1)

Based on the simulation results, Fig. 8 plots the signum function of incremental power at both ends, sgn (ΔPM) and sgn (ΔPN), and their sum (ssgn), for rectifier-side DC fault DF_1.From the signum curve, sgnum(ΔPM) and sgn(ΔPN) have opposite signs, and ssgnum reaches zero in 3 ms for DF_1.

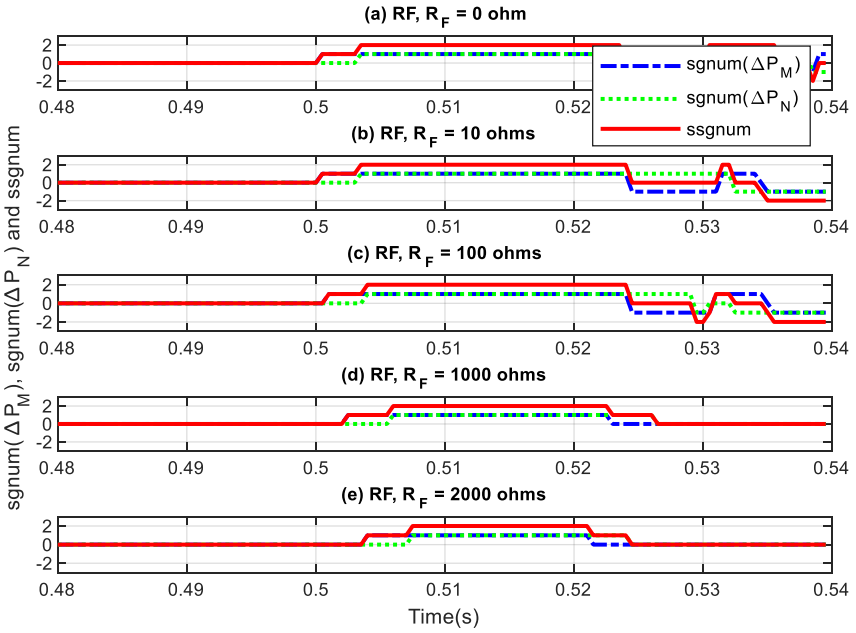


Figure 8. Performance evaluation curves for DF_1

5.2 Mid-point DC Fault (DF_2)

Fig. 9 illustrates the signum function of incremental power, expressed through sgnum(ΔPM), sgnum(ΔPN), and their combined value (ssgnum), for the case of a mid-point DC fault (DF2) across all fault resistance levels.

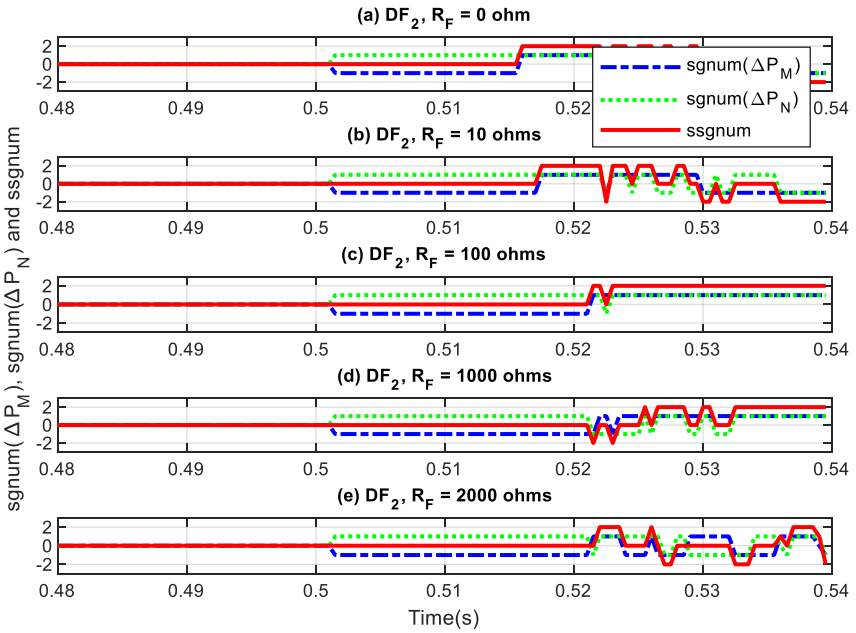


Figure 9. Performance evaluation curves for DF_2

Response curves are similar for all values of fault resistances from 0 ohms to 2000 ohms. As shown in the figure, sgnum(ΔP_M) becomes -1 and sgnum(ΔPN) becomes +1, making sgnum 0 in 1.5 ms and classifying it as an internal DC fault.

5.3 Inverter-side DC Fault (DF_3)

Similar to the signum curves obtained for rectifier-end DC faults, sgnum(ΔPM) and sgnum(ΔPN) attain opposite signs, and ssgnum reaches zero in 3 ms for inverter-end DC line faults (DF3), as shown in Fig. 10.

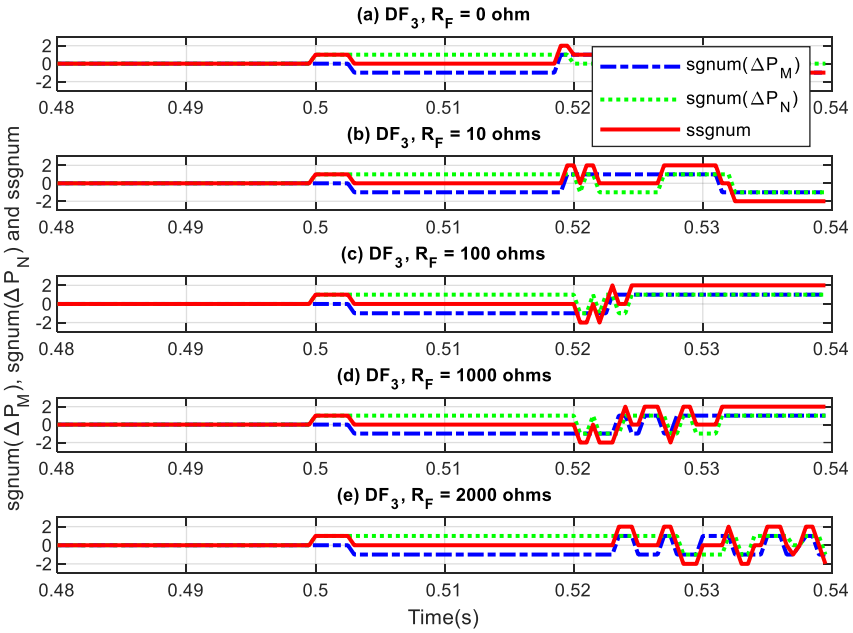


Figure 10. Performance evaluation curves for DF_3

5.4 Rectifier-side AC Fault (RF)

As shown in Fig. 11(a), for a rectifier-end AC line fault (RF) with fault resistance RF = 0 ohm, sgnum(ΔP_M) becomes +1 on fault inception, and sgnum(ΔP_N) attains +1 after a total delay time of 4 ms, and hence ssgnum changes to +2 (pointing to an external rectifier-side AC fault) in 4 ms.

Figs. 11(b) to (e) show a similar response, with classification time increasing progressively from 4 ms for RF=10 ohms to 7 ms for RF=2000 ohms. All faults in this case, for all values of fault resistance, are, however, classified by the algorithm as external rectifier-side AC faults.

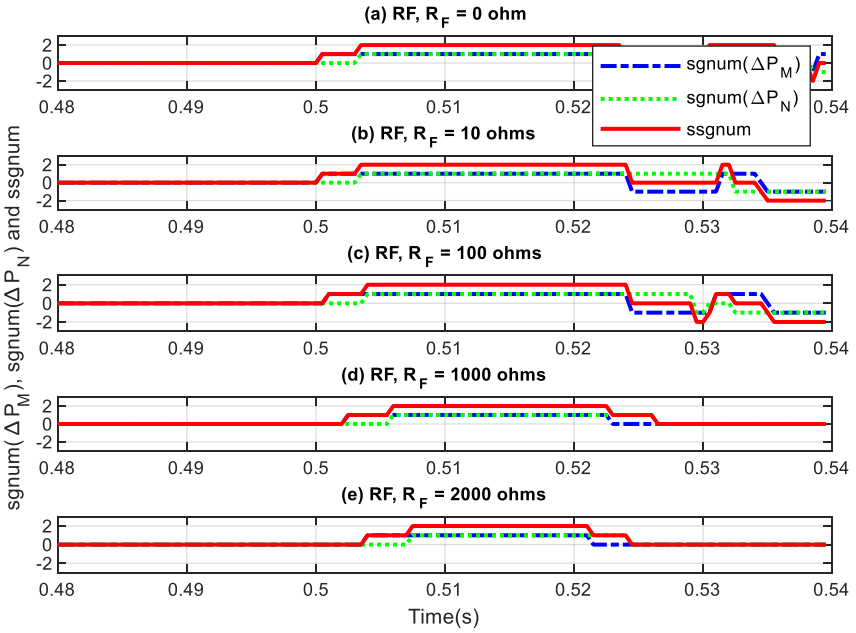


Figure 11. Performance evaluation curves for RF

5.5 Inverter-side AC Fault (IF)

Fig. 12 plots the performance evaluation curves for inverter-end AC faults in the form of sgnum(ΔPM), sgnum(ΔPN), and ssgnum.

Based on Fig. 12(a), it can be observed that sgnum(ΔP_M) reaches -1 3 ms after fault initiation, and sgnum(ΔP_N) reaches -1 at fault initiation. Therefore, at 3 ms, both ssgnum(ΔP_M) and ssgnum(ΔP_N) become -1, resulting in ssgnum becoming -2 and staying -2 for at least one AC power cycle.

In a similar manner, as depicted in Figs. 12(b) and 12(c), the fault identification times corresponding to 10-ohm and 100-ohm fault resistance are 10 ms and 12 ms, respectively. Incremental power fails to recognize faults with 1000-ohm and 2000-ohm resistance values, as illustrated in Figs. 12(d) and 12(e).

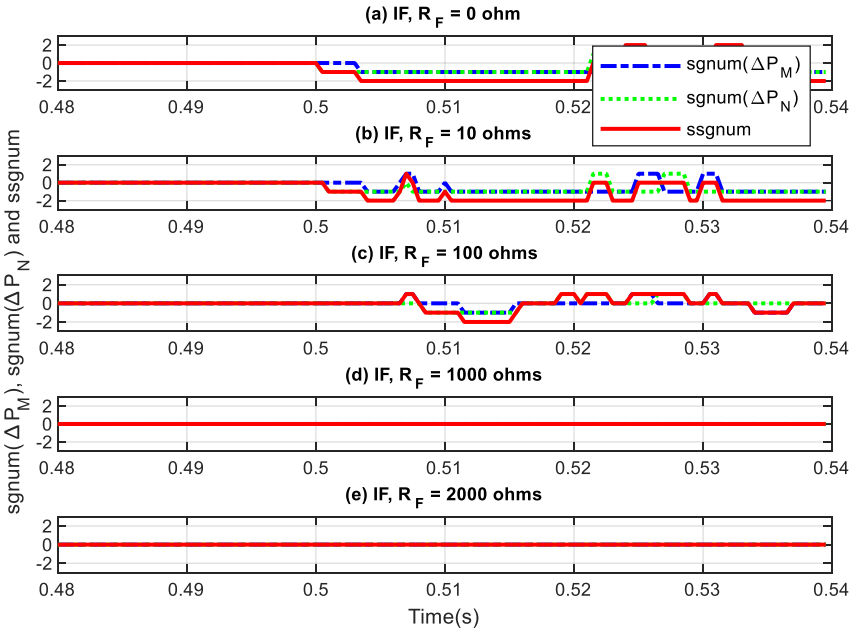


Figure 12. Performance evaluation curves for IF

6. Summary and Conclusion

Table I summarizes fault detection and classification times for all five fault locations, as well as the five fault resistance values for each location. The fault classification is accurate in all but the final two occurrences, as can be seen from the table's second-to-last column. As shown in the last column, it takes 1.5-3 ms to identify and classify transmission line faults across all fault resistance values. As mentioned earlier, this is the time it takes for a disturbance to propagate from the fault point to the relay point through the conductor and insulation materials. However, as the fault resistance varies from 0 to 2000 ohms, the proposed algorithm takes 4 to 7 ms to classify rectifier-side external faults. Similarly, as fault resistance changes from 0 to 100 ohms, the time required to classify an external inverter fault increases from 4 to 12 ms. When the fault resistance is 1000 ohms or higher, the algorithm cannot identify it as an inverter-side external fault, partly because dielectric materials and the distortion they introduce affect the signal. These detection and classification times do not include transmission delay, but the physical properties of line materials, insulation

materials, and magnetic core materials in reactors all contribute to propagation characteristics. Therefore, classification accuracy depends not only on algorithmic design but also on the electrical and thermal limits of the materials used in HVDC transmission systems.

Fault Condition	Fault Resistance (R_F) /Ω	sgnum (ΔE_M)	sgnum (ΔE_N)	ssgnum	Detection & Classification	DetectionTime (ms)	Effect of Dielectric materials
No-fault	-	0	0	0	No-Fault	-	
Internal Fault	0-2000	-1	1	0	DC Line Fault	3	Minimal effect; conductor materials dominate
	0-2000	-1	1	0	DC Line Fault	1.5	
	0-2000	-1	1	0	DC Line Fault	3	
Rectifier Fault	0	1	1	2	Rectifier Fault	4	Slight delay due to dielectric permittivity
	10	1	1	2	Rectifier Fault	4	
	100	1	1	2	Rectifier Fault	4	
	1000	1	1	2	Rectifier Fault	6	
	2000	1	1	2	Rectifier Fault	7	
Inverter Fault	0	-1	-1	-2	Inverter Fault	4	Strong influence; dielectric losses reduce sensitivity
	10	-1	-1	-2	Inverter Fault	10	
	100	-1	-1	-2	Inverter Fault	12	
	1000	0	0	0	No-Fault	Incorrect Classification	Dielectric losses attenuate and distort fault indicators
	2000	0	0	0	No-Fault	Incorrect Classification	

Table I. Summary of performance of incremental-power-based protection algorithm.

The dielectric materials of the transmission line also influence detection and classification times. At lower fault resistance values, conductor materials dominate the response, but as resistance increases, dielectric materials introduce attenuation and leakage effects that reduce sensitivity, particularly for inverter-side AC faults.

Table II compares the proposed technique with strategies examined in this work and the literature. The range of fault-resistance values, sensitivity to fault distance from the relay point, and operating duration are all compared. With fault resistance values ranging from 0 to 2000 ohms, the proposed method can detect faults anywhere along the DC transmission line. However, when the

HVDC system is connected to weak AC grids, such as those of offshore wind farms, further investigation is warranted.

Table II. Comparison of the proposed technique with strategies reported in the literature

Parameters of Protection	Proposed Technique	Ref [50] Franca et al.	Ref [3] Ma et al.	Ref [51] Liu et al.	Ref [52] Chu et al.
Operating Time	<=3 ms	< 15 ms	< 30 ms	Not presented	Not presented
Susceptibility to fault resistance (R_F)	Insensitive between 0 and 2000 ohms	Effect of fault resistance has not been explored	Insensitive between 0 and 500 ohms (higher values have not been explored)	Insensitive between 0 and 600 ohms (higher values have not been explored)	Insensitive between 0 and 600 ohms (higher values have not been explored)
Effect of fault distance on relay performance	Sensitivity maintained	Not studied	Not studied	Not studied	Not studied

Declarations

Funding: The authors declare that they received no funds, grants, or other support during the preparation of this manuscript.

Competing interests: The authors have no relevant financial or non-financial interests to disclose.

Author contributions: All authors contributed to the study conception and design. Soma Deb, Abhay Yadav, and Sumanlata Dhar performed the simulation and analysis. Soma Deb wrote the first draft of the manuscript, and all authors commented on previous versions of the manuscript. All authors read and approved the final manuscript.

Ethics approval: Not applicable. This study is based entirely on computer simulations of the CIGRE HVDC benchmark system in PSCAD/EMTDC and does not involve human participants, human data, animals, or biological material.

Consent to participate: Not applicable, as the study did not involve human participants.

Consent to publish: Not applicable, as the manuscript contains no personal data or images.

Data availability: All data generated or analysed during this study using PSCAD software are included in this published article.

.

References

1. Wang, J.; Huang, M.; Fu, C.; Li, H.; Xu, S.; Li, X. A new recovery strategy of HVDC system during AC faults. *IEEE Transactions on Power Delivery*. **2019**, 34(2), 486-495. doi.org/10.1109/TPWRD.2019.2892410

2. Muniappan, M. A comprehensive review of DC fault protection methods in HVDC transmission systems. *Protection and Control of Modern Power Systems.* **2021,** 6, 1. doi.org/10.1186/s41601-020-00173-9

3. Ma, R.; Chen, Y.; Wen, M.; Han, K. A single-ended high-impedance fault protection scheme for hybrid HVDC transmission lines based on coordination of control objectives—Journal *of Electrical Power & Energy Systems.***2024***,* 161. https://doi.org/10.1016/j.ijepes.2024.110187

4. Jin, X.; Ma, Z.; Song, G.; Gao, S. Novel pilot protection principle for high-voltage direct current transmission lines based on fault component current characteristics. *IET Generation, Transmission & Distribution.* **2015**, 5, 468-474. doi.org/10.1049/iet-gtd.2014.0313
5. Xiao, H.; Li, Y.; Liu, R.; Duan, X. Single-end time-domain transient electrical signals-based protection principle and efficient setting calculation method for LCCHVDC lines. *IET Generation Transmission and Distribution*. **2017,** 11(5), 1233–42. doi.org/10.1049/iet-gtd.2016.1159

6. Liu, L.; Liu, Z.; Popov, M.; Palensky, P.; Meijden, M.A.M.M.V.D. A fast protection of multi-terminal HVDC system based on transient signal detection. *IEEE Transactions on Power Delivery*. **2021**, 36(1), 43-51. doi.org/10.1109/TPWRD.2020.2979811

7. Leterme, W.; Azad, S.P.; Hertem, D.V. A local backup protection algorithm for HVDC grids. *IEEE Transactions on Power Delivery*. **2016**, 31(4), 1767-1775. doi.org/10.1109/TPWRD.2016.2543306

8. Leterme, W.; Barnes, M.; Hertem, D. V. Signal processing for fast fault detection in HVDC grids. *CSEE Journal of Power and Energy Systems*. **2018**, 4(4), 469-478. doi.org/10.17775/CSEEJPES.2016.00300

9. Heidary, A.; Radmanesh, H.; Rouzbehi, K.; Pou, J. A DC-Reactor-Based Solid-State Fault Current Limiter for HVDC Applications. *IEEE Transactions on Power Delivery.* **2019**, 34(2), 720-728. doi.org/10.1109/TPWRD.2019.2894521

10. Suonan, J.; Zhang, J.; Jiao, Z.; Yang, L.; Song, G. Distance protection for HVDC transmission lines considering frequency-dependent parameters. *IEEE Transactions on Power Delivery*. **2013,** 28(2), 723–732.
doi.org/10.1109/TPWRD.2012.2232312

11. Kong, F.; Hao, Z.; Zhang, S.; Zhang, B. Development of a Novel Protection Device for Bipolar HVDC Transmission Lines. *IEEE Transactions on Power Delivery*. **2014**, 29(5), 2270-2278.
doi.org/10.1109/TPWRD.2014.2305660

12. Liu, J.; Tai, N.; Fan, C.; Yang, Y. Transient measured impedance-based protection scheme for DC line faults in ultra-high-voltage direct-current system. *IET Generation Transmission and Distribution*. **2016**, 10(14),3597–3609.
doi.org/10.1049/iet-gtd.2016.0408

13. Zheng, J.; Wen, M.; Chen, Y.; Shao, X. A novel differential protection scheme for HVDC transmission lines. *International Journal of Electrical Power & Energy Systems***. 2018**, 94, 171- 178.
doi.org/10.1016/j.ijepes.2017.07.006

14. Farshad, M.; Detection and classification of internal faults in bipolar HVDC transmission lines based on K-means data description method. *International Journal of Electrical Power & Energy Systems*. ***2019***, 104,615-625.
doi.org/10.1016/j.ijepes.2018.07.044

15. Ha, H.; Yu, Y.; Yi, R.; Bo, Z.Q.; Chen, B. Novel scheme of traveling wave-based differential protection for bipolar HVDC transmission lines. *International Conference on Power System Technology*, China. **2010**, IEEE, 1-6.
doi.org/10.1109/POWERCON.2010.5666376

16. Gao, S.; Liu, Q.; Song, G. Current differential protection principle of HVDC transmission system. *IET Generation Transmission and Distribution*. **2017,** 11(5), 1286–1292.
doi.org/10.1049/iet-gtd.2016.1380

17. França, R. L. D. S.; Junior, F. C. D. S.; Honorata, T. R.; Rebeiro, J. P. G.; Costa, F. B.; Lopes, F. B.; Strunz, K. Traveling Wave-Based Transmission Line Earth Fault Distance Protection. *IEEE Transactions on Power Delivery*, **2021**, 36(2), 544- 553.
doi.org/10.1109/TPWRD.2020.2984585

18. Júnior, F. M. D. M.; Lopes, F. B. Mathematical Study on Traveling Waves Phenomena on Three-Phase Transmission Lines – Part II: Reflection and Refraction Matrices. *IEEE Transactions on Power Delivery*. **2022**, 37(2), 1161-1170.
doi.org/10.1109/TPWRD.2021.3077730

19. S. Deb and H.K. Verma, "Incremental current-based fault detection and classification in LCC-HVDC transmission system," in 2022 IEEE Delhi Section Conference (DELCON), New Delhi, India, Feb. 2022, pp. 1–6
doi: 10.1109/DELCON54057.2022.9753572.

20. S. Deb, S. Lata, V. Bhadoria, S. Tiwari, T. I. Maris, V. Vita, and G. Fotis, "Improved relay algorithm for detection and classification of transmission line faults in monopolar HVDC transmission system using signum function of transient energy," IEEE Access
doi: 10.1109/ACCESS.2022.3356012

21. Zheng, X.; Nengling, T.; Guangliang, Y.; Haoyin, D. A transient protection scheme for HVDC transmission line. *IEEE Transactions on Power Delivery*. **2012,** 27(2), 718-724.
doi.org/10.1109/TPWRD.2011.2179321

22. Kang, S.H. Current Restrained DC under-voltage protection for a bipolar HVDC system. *Journal of Engineering*. **2018**, (15), 944-949.
doi.org/10.1049/joe.2018.0279

23. Shu, H.; Wang, S.; Lei, S. Single-ended protection method for hybrid HVDC transmission line based on transient voltage characteristic frequency band. *Protection and Control of Modern Power System*, **2023**, 8, 26, 1-11.
doi.org/10.1186/s41601-023-00301-1

24. Liu, J.; Tai, FN.; Fan, C. Transient-voltage-based protection scheme for DC line faults in the multiterminal VSC-HVDC system. *IEEE Transactions on Power Delivery*. **2017**, 32(3), 483–1494.
doi.org/10.1109/TPWRD.2016.2608986

25. Zheng, X.; Nengling, T.; Guangliang, Y.; Haoyin, D. A transient protection scheme for HVDC transmission line. *IEEE Transactions on Power Delivery.* **2012**, 27,2, 718-724.
doi.org/10.1109/TPWRD.2011.2179321

26. Yang, Y.; Tai, N.; Fan, C.; Yang, L.; Chen, S. Resonance frequency-based protection scheme for ultra-high-voltage direct-current transmission lines. *IET Generation Transmission and Distribution*. **2018**, 12(2),318–327.
doi.org/10.1049/iet-gtd.2017.0488

27. Fernandes, P.C.; Honorato, T.R.; Lopes, F.V.; Silva, K.M.; Gonçalves, H.N.G.V. Evaluation of traveling wave-based fault location methods applied to HVDC systems. *Electric Power Systems Research*. **2020,** 189, 1-8.
doi.org/10.1016/j.epsr.2020.106619

28. Lopes, F.V. Settings-free traveling-wave-based earth fault location using unsynchronized two-terminal data. *IEEE Transactions on Power Delivery***, 2016**, 31(5), 2296-2298.
doi.org/10.1109/TPWRD.2016.2551367

29. Lopes, F.V.; Dantas, K.M.; Silva, K.M.; Costa, F.B. Accurate two-terminal transmission line fault location using traveling waves. *IEEE Transactions on Power Delivery*. **2017**, 33, 2, 873-880.
doi.org/10.1109/TPWRD.2017.2711262

30. Zhao, Z.; Lan, T.; Xiao, H.; Li, Y. Wavefront rising time-based traveling wave protection for multi-terminal VSC-HVDC grids. *International Journal of Electrical Power & Energy Systems*, 2023,144.
doi.org/10.1016/j.ijepes.2022.108534

31. Pourmirasghariyan, M.; Zarei, S.F.; Hamzeh, M.; Blaabjerg, F. A.; Power Routing-Based Fault Detection Strategy for Multi-Terminal VSC-HVDC Grids. *IEEE Trans Power Delivery*. 2023,38, 1,528–40.
doi.org/10.1109/ TPWRD.2022.3194420

32. Tsotsopoulou, E.; Karagiannis, X.; Papadopoulos, T.; Chrysochos, A.; Dy´sko, A.; Tzelepis, D. Protection scheme for multi-terminal HVDC system with superconducting cables based on artificial intelligence algorithms. *International Journal of Electrical Power & Energy Systems*. **2023**, 149.
doi.org/10.1016/j.ijepes.2023.109037

33. Zhang, Y.; Wang, S.; Liu, T. A waveform-similarity-based protection scheme for the VSC-HVDC transmission lines—International *Journal of Electrical Power & Energy Systems*, **2023**, 144. doi.org/10.1016/j.ijepes.2022.108571

34. Zheng, Y.; He, J.; Li, B.; Wu, T.; Dai, W.; Li, Y. Research on DC Protection Strategy in Multi-Terminal Hybrid HVDC System. *Engineering*. **2021**, 7, 1064–75.
doi.org/10.1016/j.eng.2021.05.002

35. R. Ma, Y. Chen, M. Wen, and K. Han, "A single-ended high-impedance fault protection scheme for hybrid HVDC transmission lines based on coordination of control objective," Int. J. Electr. Power Energy Syst., vol. 161, 2024.
doi: 10.1016/j.ijepes.2024.110187

36. R. H. Chandio, M. M. A. Shah, A. A. Memon, K. H. Ali, J. B. Soomro, B. Alamri, A. A. Althobaiti, and M. Alqarni, "Fault current handling in large-scale MMC-HVDC systems: an improved approach with DC circuit breaker and fault current limiter," *Front—Energy Res.*, vol. 13, 2025.
doi: 10.3389/fenrg.2025.1430142

37. Fault Detection, Classification, and Location in HVDC Transmission Lines using traveling wave theory and Hilbert transform," *IEEE Trans. Power Del.*, 2025.
https://10.1109/SGC69320.2025.11372389

38. A. Sharma, B. Li, and C. Nguyen, "Enhancing HVDC transmission line fault detection using adaptive thresholding and signal processing," Nature Energy, vol. 10, no. 2, pp. 123–134, Feb. 2025
doi: 10.1038/s41560-025-01234-x.

39. X. Zhang, Y. Kumar, and M. Andersson, “Traveling wave differential protection technology and its application in HVDC grids,” IEEE Trans. Power Del., vol. 40, no. 1, pp. 56–67, Jan. 2025
doi: 10.1109/TPWRD.2025.1234567.

40. J. Patel, L. Wang, and S. Müller, “A novel protection scheme for HVDC transmission lines based on line-mode current time warp edit distance (TWED),” Springer Electr. Eng. J., vol. 114, no. 3, pp. 245–258, Mar. 2025
doi: 10.1007/s00202-025-01234-5.

41. Y. Zhang, L. Wang, and H. Li, "A novel protection scheme for HVDC transmission lines based on line-mode current time warp edit distance (TWED)," Electrical Engineering, vol. 107, no. 2, pp. 567–580, 2025
doi: 10.1007/s00202-025-XXXXX.

42. H. B. Lima, D. Fernandes Jr., W. L. A. Neves, and R. L. A. Reis, “A new traveling wave-based methodology to optimally detect faults in HVDC systems,” SBA J. Automatics, 2025.
doi: 10.1007/s40313-025-01195-0

43. M. Nazir, J. H. Enslin, J. McCalley, and E. Hines, “Multi-terminal HVDC networks for offshore energy integration: technical challenges and grid interfacing strategies,” Energies, vol. 18, no. 24, 6383, 2025.
doi: 10.3390 /en18246383

44. R. Pan, Y. Nie, W. Huang, and Y. Liu, "Single-ended fault location of MMC-HVDC lines incorporating traveling waves," IEEE Transactions on Power Delivery, vol. 40, no. 1, pp. 123–134, Jan. 2025
doi: 10.1109/TPWRD.2025.3650205.

45. Faruque, M.O.; Zhang, Y.; Dinavahi, V. Detailed modeling of CIGRE HVDC benchmark system using PSCAD/EMTDC and PSB/SIMULINK. *IEEE Transactions on Power Delivery***. 2006**, 21, 1, 378-387.
doi.org/10.1109/TPWRD.2005.852376

46. Fei, K.; Hao, Z.; Zhang, B.H. A novel traveling wave based main protection scheme for ±800 kV UHVDC bipolar transmission lines. *IEEE Transactions on Power Delivery*. **2016,** 31,5, 2159-2168.
doi.org/10.1016/j.ijepes.2018.01.048

47. Hao, W., Mirsaeidi, S., Kang, X., Dong, X. & Tzelepis, D. A novel traveling-wave-based protection scheme for LCC-HVDC systems using Teager energy operator. *International Journal of Electrical Power and Energy Systems.* **2018,** 99, 1, 474-480.
doi.org/10.1016/j.ijepes.2018.01.048

48. Luo, S.; Dong, X.; Shi, S.; Wang, B. A directional protection scheme for HVDC transmission lines based on reactive energy. *IEEE Transaction on Power Delivery*. **2016,** 31,2, 559-567. doi.org/10.1109/TPWRD. 2015.2461450

49. Dutta, P.; Esmaeilian, A.; Kezunovic, M. Transmission-line fault analysis using synchronized sampling. *IEEE Transactions on Power Delivery* **. 2014**, 29, 2, 942-950. doi.org/10.1109/TPWRD.2013.2296788

50. França, R.L.S.; Silva, F.C. ; Costa, F.B.; Strunz,K.; Rajapakse, A.D. One-terminal traveling wave-based transmission line protection for LCC-HVDC systems. *Electric Power Systems Research*. **2023**, 223,1-8. doi.org/10.1016/j.epsr.2023.109650

51. Liu, Z.; Gao, H.; Luo, S. Non-unit protection for long-distance LCC-HVDC transmission lines based on waveform characteristics of voltage traveling waves. *International Journal of Electrical Power and Energy Systems.* **2023,** 150. doi.org/10.1016/j.ijepes.2023.109079

52. Chu, B.; Li, H.; Liang, Y.; Zhang, Q.; Peng, G.; Wang, G. Pilot protection for hybrid multi-terminal HVDC transmission lines based on Euclidean distance between differential current and distributed capacitance current. *Electric Power Systems Research*. **2023**, 224. doi.org/10.1016/j.epsr.2023.109752